

DRAFT μ FLU10-XX

PUMPING AND MIXING IN BIOMIMETIC CILIA GENERATED FLOWS

A. R. Shields^{1*}, B. Fiser², B. Evans³, M. Falvo⁴, S. Washburn⁵ and R. Superfine⁶

¹ US Naval Research Lab, Center for Bio/Molecular Science & Engineering, Washington, DC 20375
adam.shields.ctr@nrl.navy.mil¹

^{2,4,5,6} Department of Physics and Astronomy, University of North Carolina, Chapel Hill, NC 27599-3255,
blcarstens@physics.unc.edu², falvo@physics.unc.edu⁴, sean@physics.unc.edu⁵, rsuper@physics.unc.edu⁶

³ Department of Physics, Elon University, Elon, NC 27244
bevans7@elon.edu³

KEY WORDS

Actuation, Nodal Flows, Transport.

ABSTRACT

Cilia are one of evolution's earliest and remarkable innovation. They serve as the primary mechanism of cells to engage with their surrounding fluid, and more complex multicellular organisms use cilia within their physiological systems to accomplish tasks such as tissue morphogenesis and fluid flows that extend through a tissue. We have studied biomimetic cilia to provide insight into their potential contributions to biological phenomena and for their use in technologies. We find that the conical beat representative of embryonic nodal cilia produce a wealth of fascinating flows. Above the tips the fluid flow is directional and displays remnants of the cilia oscillation, both phenomena explained by analytical solutions. Below the tips we observe enhanced mixing separated from the directional flows by less than 5 microns. This mixing comes from a parameterization of the positional displacements and shows effective diffusion constants over 25 times expected from thermal diffusion. A study of the velocity distributions reveals long tails indicative of Levy flights, where unexpectedly fast long range transport can occur.

1. INTRODUCTION, BIOMIMETIC CILIA FOR PUMPING AND MIXING

Much of biology also takes place in a liquid, and as such biology provides inspiration on how to effectively interact with fluids at the microscale in the form of the cilium and flagellum [1]. These whip-like, motile structures are evolutionary biology's answer to the question of how to interact with fluids at the cellular level and are thus found in an astonishing array of biological systems. Yet, the function of cilia and flagella requires moving parts! In fact, the cilium could be considered a shining example of the fundamental moving parts of the cell: the ATP driven transport of molecular motors along microtubules. The constraints imposed by current fabrication techniques at this scale preclude a mimic with internal machinery, and so the material our biomimetic cilia are constructed from must combine the flexibility required to deform with the ability to respond to an external stimulus. Our solution to these issues has been the template-based microfabrication of a polymer-magnetic nanoparticle composite material to form free-standing arrays of magnetically actuated cilia[2].

We show that our biomimetic cilia can generate uniform, directional fluid flow by mimicking the beat shape of embryonic nodal cilia [3]. With this specific beat shape, the flow above the cilia tips is a superposition of epicycles with an overall uniform background flow. Upon actuation, the cilia generate fluid flow dramatically different below the cilia tips than above, and the transition between these two regimes occurs over a length of a few microns. While above the cilia tips the tracer motion is typically a small

epicyclic perturbation on any background flow, just below the tips the tracer pathlines show rapid fluctuations in speed and direction. Despite the overall rapidity of the flow, however, the average motion of many tracers over an area shows that the flow is still non-directional. Thus, with this nodal cilia beatshape we find that cilia can generate simultaneous, spatially segregated regimes of pumping and mixing with a distinct transition at the height of the cilia tips [4].

Beyond the observation of phenomena, we seek to understand the cilia generated flows with quantitative models. We show that the flows above the tips is described by a combination of Poiseuille, Couette and Stokes 2nd problem flows [5]. For the flows below the cilia tips, we present these results within the context of cilia-generated mixing via an effective diffusivity and Lévy flight distributions [6].

2. PUMPING AND DIRECTED FLOW ABOVE THE CILIA TIPS

In our system we find that flow above the cilia tips has an average velocity that depends upon the height in the channel thereby providing a pumping function for microfluidic flows. The localized nature of the structure-fluid interaction produces localized epicyclic orbits whose magnitude decays with distance above the tips. When the flow is time averaged, the flow follows from a combination of canonical shear and pressure driven boundary conditions.

2.1 The flow varies with height according to canonical boundary conditions

The tilted conical beat produces a time averaged flow in the direction of the motion of the cilia tip at its highest point. Although the tip does move in the backward direction during its return cycle, this motion is

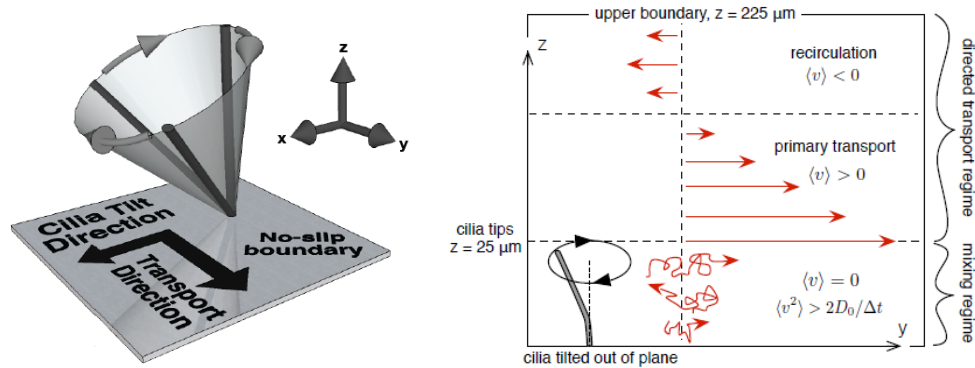


Figure 1: A cilium is actuated by a magnetic field to precess on a tilted cone (Left). This produces flows that depend on the location of the fluid with respect to the cilia tips. Above the tips the flow, on average, is in the direction of the tip velocity at the top of its motion. In our case, with a closed lid, the flow can be retrograde near the top of the chamber. Below the tips the flow has the hallmarks of diffusive mixing with little time averaged flow.

closer to the chamber floor, and the no-slip boundary condition of the floor ensures that the flow induced by the tip during the return stroke will generate less flow [7]. The oscillatory shear at the height of the cilia tips suggests a shear boundary condition at that location. Further, our chamber is closed, so no net pumping can occur. This accounts for the return flow that we observe well above the cilia tips near the top of the closed channel. This flow can be accounted for by assuming a pressure driven flow in the return direction. The combination of these results in a function form for Poiseuille-Couette flow that can be fit to the flow profile:

$$u(z) = \frac{u_0}{h}(h-z) + \frac{\nabla P}{2\eta}(z^2 - hz) \quad (1)$$

Where u is the fluid velocity, h is the channel height, η is the solution viscosity and p is the pressure. This functional form fits our microchannel flow profiles with biomimetic cilia. Most significant is that this form also fits the data from the nodal plate of a developing embryo. The flow within this structure has been shown to be responsible for the left-right asymmetry of vertebrates. In previous work we have fit this model to the limited biological measurements taken in a mouse embryo by Okada et al. (2005) [3].

2.2 The flow is epicyclic, superimposed on directional flow.

Closer examination of the tracer paths reveals an oscillatory component that adds to a directional component [8]. We seek to understand whether the oscillatory nature of these epicycles can be understood within the

context of the oscillatory motion of a continuous boundary. Hence we consider the superposition of the modified form of Stokes 2nd problem with Couette flow.

$$u(y,t) = \text{Re} \left[U e^{i\omega t} \frac{\sinh \left[\frac{\delta_o}{A} (h-y) \right]}{\sinh \left[\frac{\delta_o}{A} h \right]} \right] + \frac{\delta_o}{h} (h-y) \quad (2)$$

where $A = U/\omega$, $\delta_o = (1+i)\sqrt{\omega/2\eta}$, and h is the height of the chamber and u_o is the velocity of the plane driving the Couette flow. To fit this model (Figure 2) to our flows we have been forced to make two ad hoc assumptions applied to two separate phenomenon in the model. Both assumptions are that the cilia interaction with the fluid is reduced by about a factor of 2 from what one would expect for a flat plane. This assumption must be applied to the cilia tip velocity in order to achieve the correct amplitude at the height of the cilia tips, and then it must be applied again as an effective viscosity in order to describe the fact that the modeled plane only interacts with the fluid over a fraction of its total area. The factor of two that we have used in both cases is approximately the same as the area fraction that the cilia trajectories occupy, as derived from an analysis of the videos of the system.

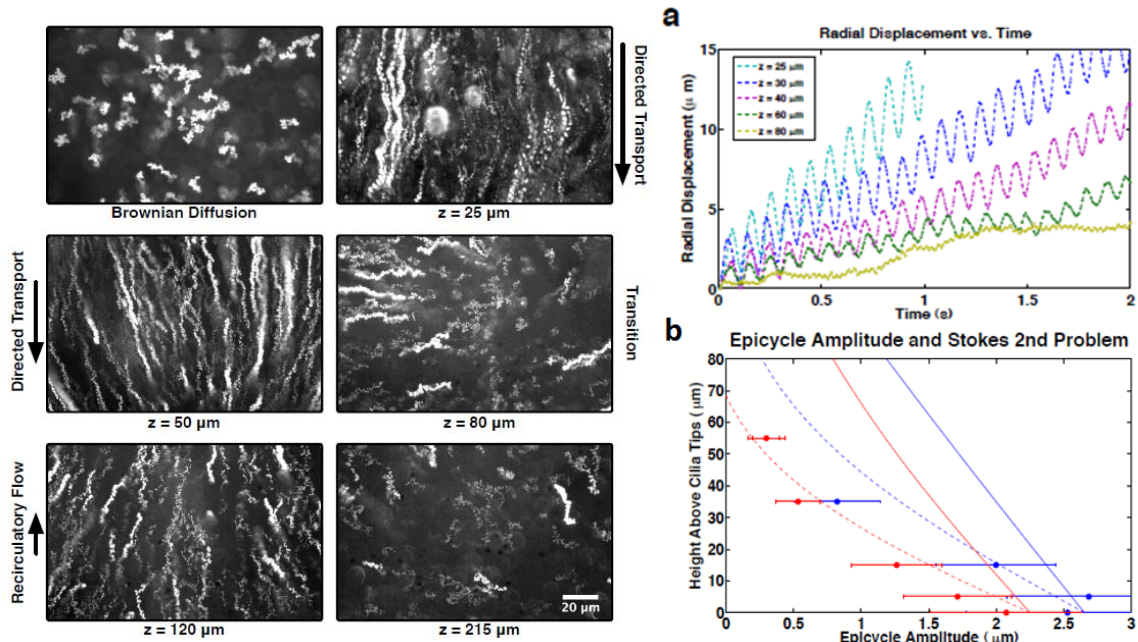


Figure 2: The flow above the cilia tips left panel) is shown as maximal projections of the video data, progressing from the height of the tips to the boundary of retrograde flow (80 microns) to retrograde flow (120 microns) to the upper fixed boundary (215 microns). The directed flows are superimposed on oscillatory motion (epicycles) due to the cilia presenting an oscillatory shear boundary condition (right panel). The epicycle amplitude is fit to an analytical flow comprised of Stokes 2nd problem and Couette flow. We plot the amplitude epicycle vs height and compare it to the amplitude from Stokes 2nd problem for two different cilia beat frequencies (red, 12 Hz and blue, 33 Hz). The solid curves are the predictions from equation 5.2 with the actual viscosity, and the dotted lines are from assuming a decreased effective viscosity. This behavior suggests that the cilia-driven motion can be thought of as Stokes 2nd problem in which the interaction strength is reduced by roughly the area fraction of the cilia.

3. MIXING BELOW: DIFFUSION AND LÉVY FLIGHTS

We now focus on the nature of the fluid flow below the cilia tips. The understanding of many biological fluid-mediated processes, and by extension the cellular systems which rely on these processes, requires an understanding of how stirring and diffusive processes interact to produce particle transport. In systems with motile cilia, the fluid-driven by the cilia motion creates stirring and results in the advective motion of the particles. Experimental studies of biological ciliated systems are often difficult to interpret due to the large number of biochemical and biophysical variables. To date there is very little experimental data on the

detailed motions of cilia-driven particles [9,10]. Furthermore, theoretical studies of ciliated systems rarely incorporate diffusion because of the added theoretical complexity, instead assuming that advective transport is sufficiently strong to dominate diffusion [11,12].

The first framework we describe is that the biomimetic cilia drive a fluid flow below their tips in which the dispersion of advected particles can be approximated as an enhanced diffusion process. The second framework falls under the umbrella of anomalous transport, which has also been referred to as strange kinetics. These terms describe dynamical systems in which the transport properties exhibit non-Gaussian statistics and Lévy flights.

3.1 Cilia driven flow between cilia can be described by enhanced diffusion

We find that the analysis of the particle positions indicates that particles may be mixed at a rate which scales in time like a diffusive process, but the rate itself is enhanced over that which would be expected from the thermal diffusivity of the particle. The expected displacement of an object exhibiting diffusive motion scales with the square root of time, much slower than ballistic motion. To evaluate the temporal evolution of transport in a given fluid flow a widely used metric is the mean square displacement (MSD) as a function of lag time τ :

$$\langle r^2 \rangle = c\tau^\gamma \quad (3)$$

This general form reduces to ballistic motion if $\gamma = 2$, in which case $c = 2v$, and reduces to diffusive motion if $\gamma = 1$, in which case $c = 2dD_0$ where d is the system dimensionality. In addition, phenomena which inhibit diffusion can lead to $0 < \gamma < 1$, which is referred to as sub-diffusive motion, while in some cases, such as turbulent flow, processes termed super-diffusive can lead to $2 < \gamma \leq 3$.

The temporal scaling of the MSD is advantageous because it will easily discriminate between the constant average velocity motion above the cilia tips and the complex, non-directional flows below the tips. However, the conventional MSD is a measure of how rapidly in time an object moves away from its initial location. To address the issue of mixing in biological ciliated systems, a more useful measure is the scaling law with which objects move away from each other. For this reason, we employ the relative dispersion, a

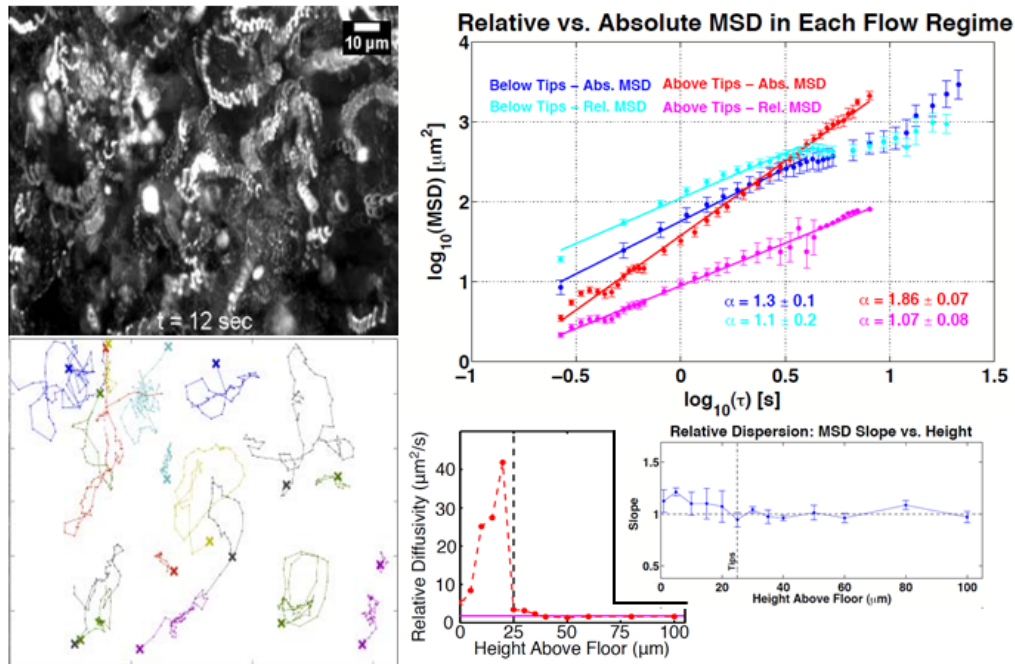


Figure 3: The flow below the cilia tips (upper left panel) is shown as a maximal projection, with the tracked trajectories shown below. Top right is the collected mean square displacement of the individual trajectories and of the two-particle relative trajectories. The latter show the motion of the particles without the directed flow component that is shared by the particles. The MSD of the individual trajectories above the tips show a power law of 2 consistent with directed flow, while the two-particle relative MSD has a power law of 1 due to its diffusive component. Lower right is show the power law for the relative trajectory MSD as a function of height, and the effective diffusion constant derived from the MSD plots.

metric of how the position of one object changes with lag time relative to other moving objects [13]. Conceptually, relative dispersion treats the time course of the separation of two objects as though it were itself a single object. It is immediately clear that the highly directional motion above the cilia tips is strongly suppressed in the separation trajectories, while below the cilia tips the trajectories retain the complexity of the originals.

Figure 3 compares the slopes of linear regressions of the single particle MSD with the MSD of the relative motion of the same tracers for the two fluid flow regimes. The single particle MSDs are as expected: below the cilia tips the complex nature of the tracer trajectories leads to a temporal scaling which is between ballistic and diffusive, while above the cilia tips the uniform directionality and relatively constant tracer speeds result in a slope which is nearly ballistic. In contrast, for both flow regimes the relative MSD has a slope of nearly 1. This implies that, although the tracer motion is cilia-driven and thus largely advective, in both regimes the temporal scaling of the separation of particles evolves diffusively. The importance of this observation is that it implies that beating cilia have the potential to generate fluidic mixing between cilia by enhancing the rate at which particles spread from each other up to a factor of approximately 25 [4].

3.2 Cilia driven flow between cilia is characterized by long tail distributions.

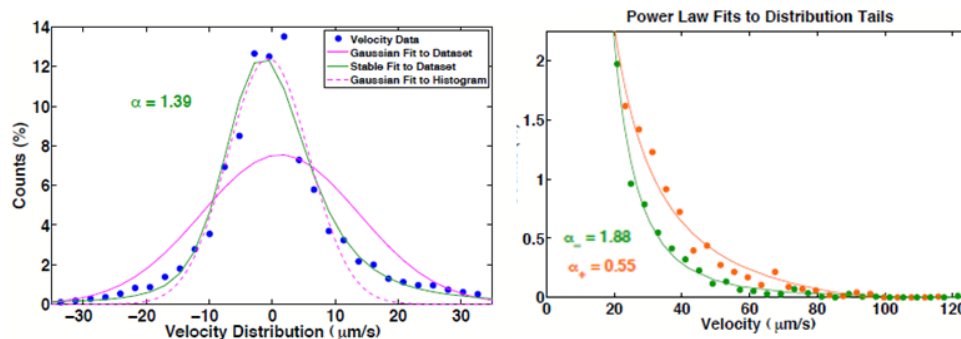


Figure 4: Velocity distributions of the cilia-driven flow exhibit non-Gaussian statistics. In (a) we plot several ways to fit a Gaussian to the distribution. The solid magenta line is the Gaussian distribution which has the same mean and standard deviation as the velocity dataset. In contrast, the dotted magenta line is a true fit to the histogram itself. Both examples show how the velocity distribution is non-Gaussian, and a stable distribution fit with $\alpha = 1.39$ matches the data well. A second method for determining α is the asymptotics of the tails of the distribution, as identified at right. Both tails are fit to a power law to determine α separately for each tail. In each case, α is less than two, indicating the velocity distributions are infinite variance and thus the particle trajectories are Lévy flights.

Looking beyond the statistics of the MSD characterization, the velocity distributions reveal further interesting insights. We find that the tracer motion below the cilia tips exhibit characteristics of Lévy flights, a type of random walk where the size of the steps trends towards a distribution with infinite variance. In Figure 4 we study the velocity distribution from particles below the cilia tips. Here we fit the distribution data to a skew normal distribution. The search for distributions with such characteristics led to the development of the Lévy skew-alpha stable distribution. This distribution is embodied by the four parameters α , β , γ , and δ . These parameters determine, respectively, the rate of decay of the distribution tails, the skewness, the scale (or width), and the location. A Gaussian distribution is equivalent to a stable distribution with α equal to 2 and $\beta = 0$. for any $\alpha < 2$ the stable distribution has infinite variance, and so such a process is scale-invariant and can be called a Lévy flight. Stable distributions with $\alpha < 2$ are also known as ‘heavy-tailed’ distributions, with larger probabilities for events to occur at the largest values in the distribution. Thus, a Lévy flight has rare, but large excursions from the small steps which are much more likely. In Figure 4 we show such a fit, demonstrating that the velocity distribution data is heavier-tailed than a Gaussian, an indication that the particles are undergoing Lévy flights [6]. We speculate that the long excursions exhibited by a Lévy flight increase the rate at which a species can explore a given area, which may have implications for biochemical signaling in ciliated systems.

5. CONCLUSIONS

Cilia are at the center of diverse biological phenomena including the clearance of the lung and the left-right asymmetry of vertebrates, to name a few. The study of the fluid flows from biomimetic cilia arrays allows us to understand the full physiological consequences of these flows, as well as consider their roles in new

technologies. We have studied the flows from our biomimetic cilia and demonstrated that directional flows occur simultaneously, but in distinct regions, from complex mixing flows. The mixing affects can be very large with effective diffusion constants above 25 times that of thermal diffusion. Detailed analysis of velocity distributions reveals long tailed distributions which may allow species to travel far from the diffusive distribution with unexpected speed.

ACKNOWLEDGEMENTS

We thank all members of the Virtual Lung Project, especially Greg Forest, Sorin Mitran, Rich McLaughlin, and Roberto Camassa for valuable discussions. We thank Russell Taylor and University of North Carolina's computer science department for assistance and development of Video Spot Tracker. Finally, we thank two anonymous referees for a number of helpful comments. The work was supported by National Aeronautics and Space Administration University Research, Engineering and Technology Institutes (NCC-1-02037), NIH (P41-EB002025-25A1), National Science Foundation Nanoscale Interdisciplinary Research Teams (CMS-0507151), National Science Foundation Research Training Groups (DMS-0502266), and the National Heart, Lung, and Blood Institute (R01-HL077546-03A2).

REFERENCES AND CITATIONS

- [1] Satir, P. and Christensen, S. T. (2007). Overview of structure and function of mammalian cilia. *Annu Rev Physiol*, 69:377-400.
- [2] Evans, B. A., Shields, A. R., Carroll, R. L., Washburn, S., Falvo, M. R., and Superfine, R. (2007). Magnetically actuated nanorod arrays as biomimetic cilia. *NanoLetters*, 7(5):1428-1434.
- [3] Okada, Y., Takeda, S., Tanaka, Y., Belmonte, J.-C. I. C., and Hirokawa, N. (2005). Mechanism of nodal flow: a conserved symmetry breaking event in left-right axis determination. *Cell*, 121(4):633-644.
- [4] Shields, A.R., Fiser, B. L., Evans, B.A., Falvo, M.R., Washburn, S., & Superfine, R. , Biomimetic cilia arrays generate simultaneous pumping and mixing regimes. *Proceedings of the National Academy of Sciences*, 2010. 107(36): p. 15670-15675.
- [5] Happel, J. and Brenner, H. (1963). *Low Reynolds number hydrodynamics*. Martinus Nijhoff, Netherlands, 3rd edition.
- [6] Shlesinger, M., Zaslavsky, G., and Klafter, J. (1993). Strange kinetics. *Nature*, 363:31-37.
- [7] Cartwright, J. H. E., Piro, N., Piro, O., and Tuval, I. (2008). Fluid dynamics of nodal flow and left-right patterning in development. *Dev Dyn*, 237(12):3477-3490.
- [8] Bouzarth, E. L., Brooks, A., Camassa, R., Jing, H., Leiterman, T. J., McLaughlin, R. M., Superfine, R., Toledo, J., and Vicci, L. (2007). Epicyclic orbits in a viscous fluid about a precessing rod: theory and experiments at the micro- and macro-scales. *Phys Rev E Stat Nonlin Soft Matter Phys*, 76(1 Pt 2):016313.
- [9] Vilfan, M., Potocnik, A., Kavcic, B., Osterman, N., Poberaj, I., Vilfan, A., and Babic, D. (2009). Self-assembled artificial cilia. *Proc Natl Acad Sci U S A*.
- [10] Supatto, W., Fraser, S. E., and Vermot, J. (2008). An all-optical approach for probing microscopic flows in living embryos. *Biophys J*, 95(4):L29-31.
- [11] Fauci, L. J. and Dillon, R. (2006). Biofluidmechanics of reproduction. *Annu. Rev. Fluid Mech.*, 38:371-394.
- [12] Smith, D. J., Gaffney, E. A., and Blake, J. R. (2007). Discrete cilia modelling with singularity distributions: application to the embryonic node and the airway surface liquid. *Bull Math Biol*, 69(5):1477-1510.
- [13] Babiano, A., Basdevant, C., Le Roy, P., and Sadourny, R. (1990). Relative dispersion in two-dimensional turbulence. *Journal of Fluid Mechanics Digital Archive*, 214:535-557.